



Microstructural evolution and creep properties of Mg–4Sn alloys by addition of calcium up to 4 wt.%

Amir BAGHANI¹, Hamid KHALILPOUR², Seyed Mahdi MIRE SMAEILI³

1. Department of Mechanical Engineering, University of Iowa, Iowa City, IA, USA;
2. Department of Mining, Metallurgical and Materials Engineering, Laval University, Québec, Canada;
3. Faculty of Mechanical Engineering, Shahid Rajaei Teacher Training University, Tehran, Iran

Received 14 March 2019; accepted 16 February 2020

Abstract: The effects of addition of calcium up to 4 wt.% on the microstructure and creep properties of Mg–4Sn alloys were investigated by the impression creep test. Impression creep tests were performed in temperature range between 445 and 475 K under normalized stresses σ/G (where σ is the stress; G is the shear modulus) between 0.0225 and 0.035. Optical microscopy and scanning electron microscopy were used to study the microstructure of samples. It is observed that the addition of Ca more than 2 wt.% suppresses less stable $MgSn_2$ phase, and instead forms more thermally stable phases of Ca–Mg–Sn and Mg_2Ca at the grain boundaries which improve the creep resistance of Mg–4Sn alloys. According to the stress exponents ($6.04 < n < 6.89$) and activation energies ($101.37 \text{ kJ/mol} < Q < 113.8 \text{ kJ/mol}$) which were obtained from the impression creep tests, it is concluded that the pipe diffusion climb controlled dislocation creep is the dominant creep mechanism.

Key words: impression creep test; Mg–Sn–Ca alloy; creep mechanism; microstructure

1 Introduction

Magnesium alloys are widely used in applications where high specific strength is required [1,2]. Among magnesium alloys, those based on Mg–Al system possess an excellent combination of superior castability, good corrosion resistance and acceptable mechanical properties at room temperature and reasonable cost [3–7]. However, the formation of $Mg_{17}Al_{12}$ intermetallic compound (with a low melting point) at lower temperature, has reduced the creep resistance at higher temperatures and restricted the applications of Mg–Al alloys [8]. In recent studies, many efforts have been carried out to improve the high temperature properties of aluminum-free magnesium alloys [9–12].

Mg–Sn based alloys drew researcher's

attention because of their structural stability at high temperatures. The maximum solidification temperature for Mg–Sn binary alloys is about 67 °C, which is much less than that for the binary alloys of Mg–Al (136 °C), and Mg–Zn (283 °C). Having shorter solidification range in Mg–Sn alloys, make it easier to produce a sound component with less shrinkage porosity and hot tear [13]. In addition, thermally stable Mg_2Sn intermetallic particles, distributed along grain boundaries, improve the high temperature properties of these alloys [14]. Moreover, Mg_2Sn phase can easily precipitate at higher temperature of 560 °C because of high solubility limit of Sn in Mg (14.48 wt.%) while it shows little solubility at lower temperatures. So, it is expected to enhance the strength at both ambient and elevated temperatures [10,15–19].

Tin has a significant role in reduction of stacking fault energy of α dendrite solid solution of

Sn in Mg [16]. The dissociation of dislocations into partial dislocations will occur easily when the stacking fault energy is reduced. Although partial dislocations glide in the planes, they are not able to climb individually. Hence, to activate the climbing process, stress is required to be increased to merge the dislocations, which means improving the creep resistance [17].

In recent studies, the addition of calcium (Ca) to the Mg–Sn alloys has been found to further improve the creep resistance of as-cast products due to the formation of Ca–Mg–Sn and Mg₂Ca phases [10,14,20–24]. In fact, Ca–Mg–Sn phase is thermally stable up to 500 °C which improves the creep resistance during compression [10,20].

NAYYERI and MAHMUDI [10] studied effects of increasing calcium level up to 2 wt.% on the impression creep behavior of the Mg–5Sn alloy. However, effects of using higher contents of Ca on the microstructure and creep resistance still require more attention. The aim of this study is to investigate the microstructure and creep properties of the Mg–4Sn–*x*Ca alloys with more than 2 wt.% Ca by employing impression creep test [25].

2 Experimental

High purity magnesium (99.9%) ingot was melted in a graphite crucible under protection of an atmosphere of air with 5% SO₂ at (750±1) °C and then high purity ingots of Sn (99.9%) and Ca (99.9%) were added to the melt. Then, the melt was poured into a steel mold preheated at 200 °C using the tilt casting method. Using this method, the melt filled the mold with the lowest possible turbulence and avoided the formation of oxide inclusion and air entrapment. The chemical compositions of the alloys, measured by optical emission spectroscopy, are shown in Table 1.

Wire electro-discharge machining was used to prepare impression creep test samples with dimensions of 10 mm × 10 mm × 6 mm. The creep tests were performed by employing the impression creep test method. This method has some major differences with conventional tensile creep test. The impression creep test is based on the pressure of a flat-ended cylindrical punch with 2 mm in radius on small sample [26]. In this method, the transient displacement of punch is recorded. In fact, the second stage of creep is investigated, while the third

stage does not exist in this method. On the other hand, since this method is pressure-based in nature, the necking and fracture of the sample will not occur. In this study, impression creep tests were performed in temperature range between 445 and 475 K under normalized stresses σ/G (σ is the stress; G is the shear modulus) between 0.0225 and 0.035. For this purpose, a SANTAM STM–20 universal tensile testing machine, equipped with a three-zone furnace, was used to perform the impression creep test. The cast samples were studied by scanning electron microscopy (SEM) and optical microscopy to examine both the as-cast microstructure and the evolution of microstructure after creep test. Microscopic studies were accomplished by employing a Litz-Mettalloplan optical microscope and a VEGA2-TESCAN scanning electron microscope equipped with EDS.

Table 1 Chemical compositions of particles in tested materials

Alloy	Particle or phase	Content/wt.%		
		Mg	Sn	Ca
Mg–4Sn	Mg ₂ Sn	60.91	39.09	–
Mg–4Sn–2Ca	Mg ₂ Ca	84.47	0	15.53
	Ca–Mg–Sn	41.1	46.33	12.57
Mg–4Sn–3Ca	Mg ₂ Ca	81.11	0	18.89
	Ca–Mg–Sn	33.71	51.03	15.26
Mg–4Sn–4Ca	Mg ₂ Ca	82.81	0	17.19
	Ca–Mg–Sn	21.72	59	19.28

3 Results and discussion

3.1 Microstructural evolution

Figure 1 shows the microstructures of the as-cast Mg–4Sn alloys with different contents of Ca. The microstructures of Mg–4Sn alloy included alpha (α) matrix phase and eutectic structure of Mg₂Sn phase at grain boundaries. By adding Ca up to 2 wt.%, dendritic structure was broken and some rod-shape phases appeared in the microstructure. According to Fig. 1, Mg₂Sn was formed at the grain boundaries of Mg–4Sn alloy, which supported previous findings in Ref. [10]. It was observed that when Ca was added to this alloy up to 2 wt.%, the Mg₂Sn disappeared and existing Sn participated during the formation of Ca–Mg–Sn phase [27]. It was shown in Figs. 1(c) and (d) that increasing the

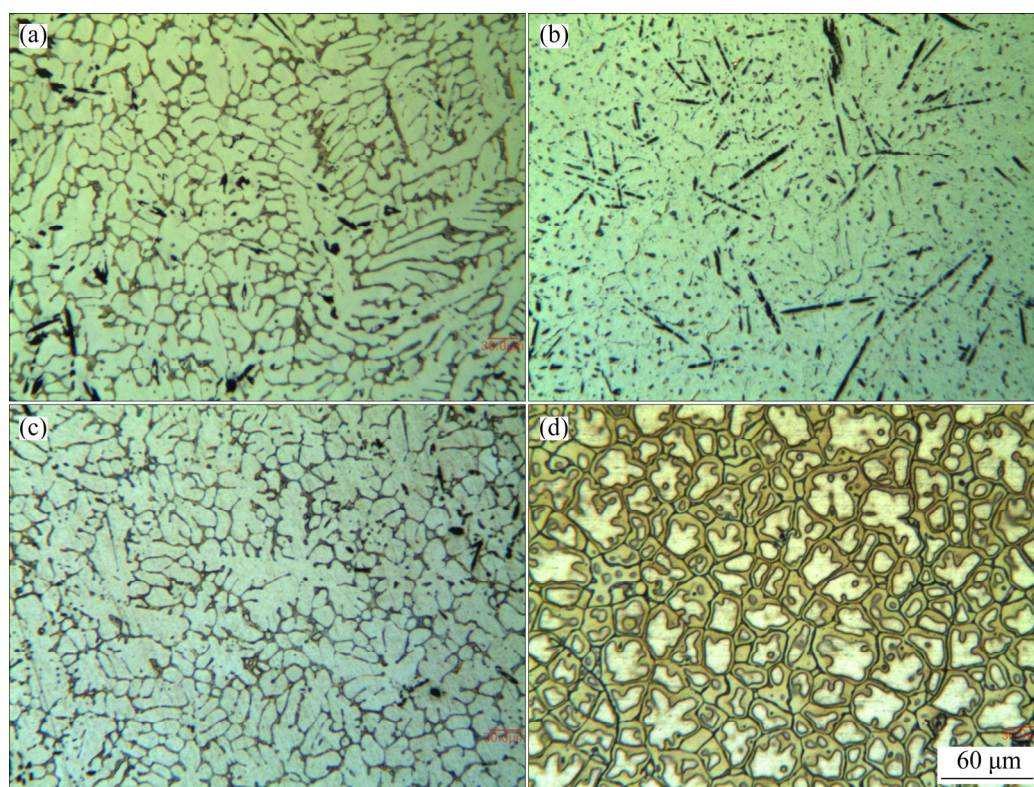


Fig. 1 Optical microscopic images of different as-cast alloys: (a) Mg–4Sn; (b) Mg–4Sn–2Ca; (c) Mg–4Sn–3Ca; (d) Mg–4Sn–4Ca

amount of Ca up to 3 and 4 wt.% increased the volume fraction of Ca–Mg–Sn phase, which formed the eutectic structure again. Figure 1 demonstrated that the continuous phase at grain boundaries was Mg_2Ca and its continuity increased by increasing the amount of Ca.

SEM micrographs were taken at higher magnifications for analyzing these phases (Fig. 2). As expected, the Mg_2Sn phase was observed at grain boundaries (bright particles and phases) where no Ca was used in this alloy (Fig. 2(a)). It could be observed in Fig. 2(b), in the alloy with 2 wt.% Ca that the eutectic phase was refined and rod-shape Ca–Mg–Sn phases were formed in the matrix. Figures 2(c) and (d) revealed that increasing the Ca content increased the continuity of Mg_2Ca phase in the interdendritic areas and along grain boundaries (gray phases).

The formation of different phases during and after the solidification was predicted by JmatPro and the results were shown in Fig. 3 for Mg–4Sn and Mg–4Sn–4Ca alloys. Analysis of Mg–4Sn alloy indicated that α magnesium dendrites were the only phase which nucleated during the solidification while Mg_2Sn was formed at 370 °C

below the solidus temperature at 636 °C (Fig. 3(a)). As expected, increasing the Ca content up to 4 wt.% in Mg–4Sn–4Ca removed the Mg_2Sn phase from the microstructure and instead Ca–Mg–Sn eutectic phase was formed at 609 °C in the mushy zone. After Mg–4Sn–4Ca alloy solidified completely, Mg_2Ca was formed at 516 °C (Fig. 3(b)). According to the JmatPro predictions (Fig. 3), increasing the Ca content in the Mg–Sn alloys removed Mg_2Sn particles and formed Ca–Mg–Sn and Mg_2Ca instead, which were in good agreement with the microscopic analysis.

3.2 Creep properties

Figure 4 exhibits typical creep curves of impression depth with respect to time, at a fixed temperature of 455 K and normalized stress of 0.0300 for four alloys. It indicates that increasing the Ca content decreases the slope of curves which is considered as the impression velocity. The same regimes in quantitative data of impression velocity for four alloys at 465 K and normalized stress of 0.0275 are shown in Table 2.

Figure 5 shows creep curves for Mg–4Sn–3Ca alloy at a fixed normalized stress of 0.0250 in the

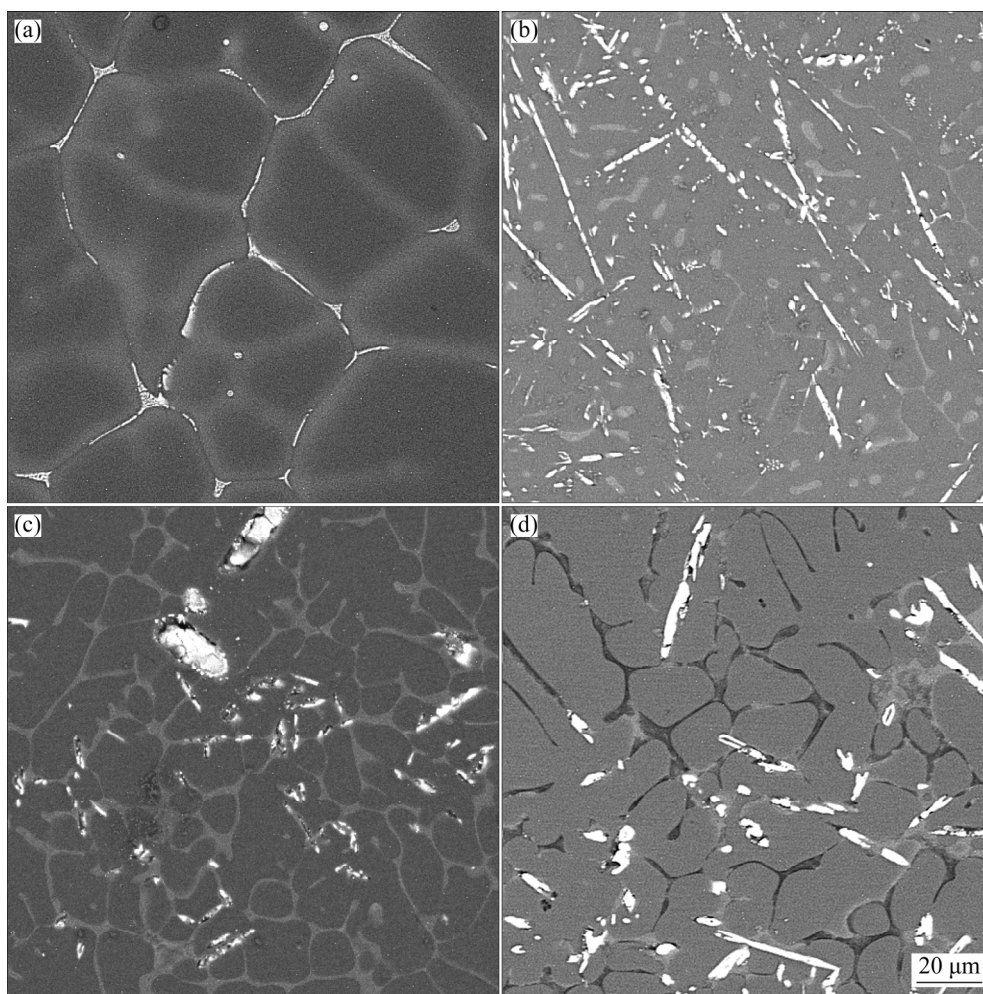


Fig. 2 SEM images of Mg-4Sn alloys with different amount of Ca: (a) Mg-4Sn; (b) Mg-4Sn-2Ca; (c) Mg-4Sn-3Ca; (d) Mg-4Sn-4Ca

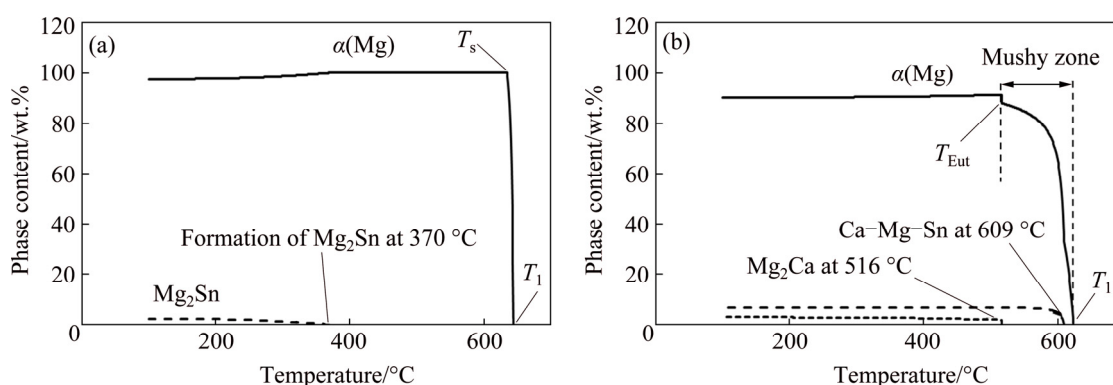


Fig. 3 Formation of different phases during and after solidification: (a) Mg-4Sn; (b) Mg-4Sn-4Ca

temperature range between 345 and 375 K. As is shown in Fig. 5, the elevation of the temperature under a constant applied stress increases penetration depth and impression rate.

The lower impression rate of Mg-4Sn-4Ca is referred to the continuity of Mg₂Ca phase at grain boundaries and the presence of high volume of

Ca-Mg-Sn phase which has a higher melting point ($T_m=1184\text{ }^{\circ}\text{C}$) than the Mg₂Sn phase ($T_m=770\text{ }^{\circ}\text{C}$) [18,28]. It is worth noting that, there is no applied heat treatment process for dissolving Ca-Mg-Sn compounds [27]. The impression creep rate, $\dot{\epsilon}^0$, was computed by taking the derivatives of the impression depth with respect to the creep time

Table 2 Obtained impression rates in creep test for four alloys at 465 K and normalized stress of 0.0275

Alloy	Impression velocity, $V_{imp}/(\text{mm}\cdot\text{s}^{-1})$
Mg-4Sn	0.107
Mg-4Sn-2Ca	0.0957
Mg-4Sn-3Ca	0.0665
Mg-4Sn-4Ca	0.0418

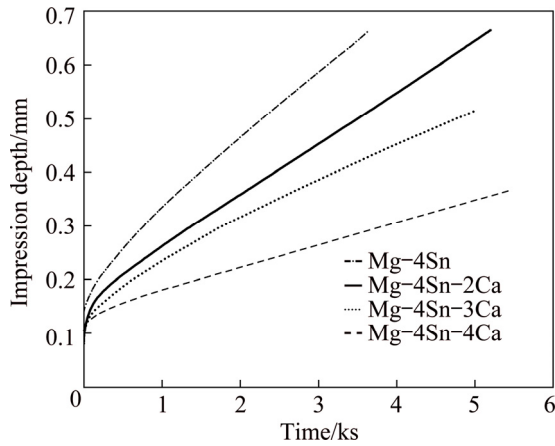


Fig. 4 Variation of impression depth with time at 455 K and normalized stress (σ/G) of 0.0300 for four alloys

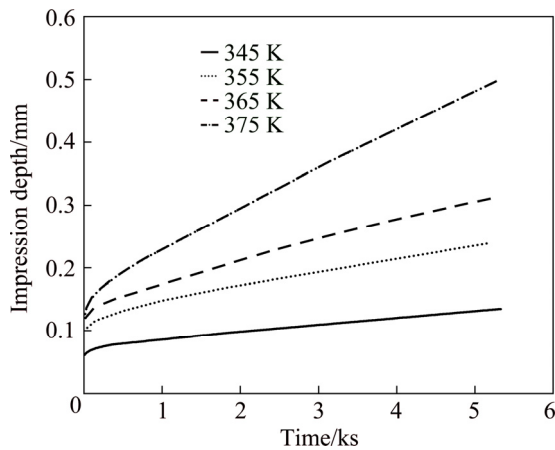


Fig. 5 Variation of impression depth with time for Mg-4Sn-3Ca at normalized stress of 0.0250 and different temperatures

and plotted in Fig. 6 for different normalized stresses. As expected, all the creep curves exhibit a primary stage in which the creep rate drops sharply with time, and then in the second stage curves follow a constant impression creep rate regime.

According to Fig. 6, impression creep rates in Mg-4Sn-4Ca alloy are lower than those of Mg-4Sn-2Ca alloy.

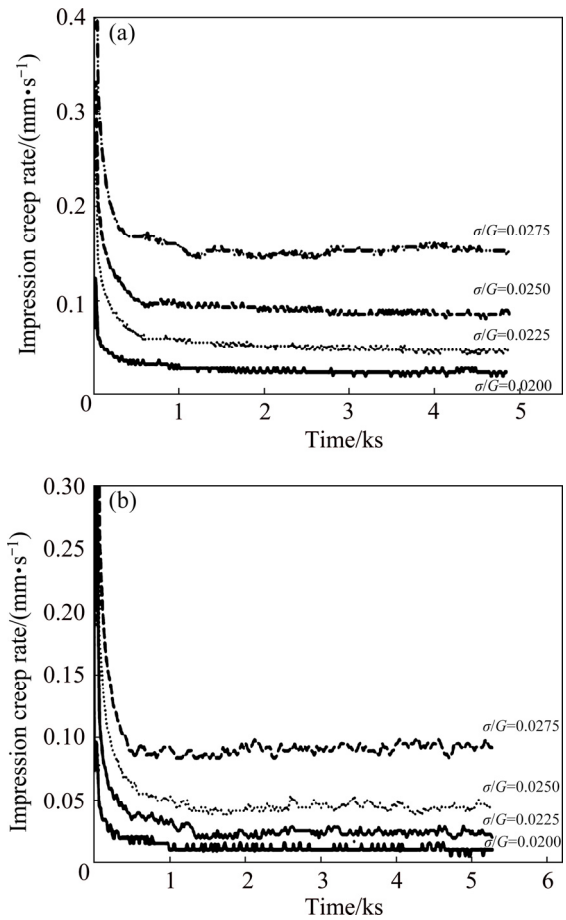


Fig. 6 Variation of impression creep rate with time for different contents of Ca at constant temperature of 475 K and different normalized stresses: (a) Mg-4Sn-2Ca; (b) Mg-4Sn-4Ca

3.3 Creep mechanism

Creep mechanism can be determined by calculating stress power n and creep activation energy Q according to Eq. (1) [8,10,20]:

$$\dot{\epsilon}^0 = A \left(\frac{b}{d} \right)^p \left(\frac{GbD_0}{KT} \right) \left(\frac{\sigma}{G} \right)^n \exp \left(-\frac{Q}{RT} \right) \quad (1)$$

where A , b , d , p , G , D_0 , K , T , σ , n , Q and R are constant, Burger’s vector component, grain size, grain size exponent, shear modulus, appropriate diffusion coefficient constant, Boltzmann’s constant, temperature, stress, stress exponent, creep activation energy and mole gas constant, respectively.

According to the last studies, the correlation between impression and tensile creep data is obtained by some substituting and rearranging in Eq. (1), therefore, the relationship between the impression velocity V_{imp} and the applied punch stress σ_{imp} is

$$\left(\frac{V_{\text{imp}}T}{G}\right) = A \left(\frac{\varphi C_2}{C_1^n}\right) \left(\frac{b}{d}\right)^p \left(\frac{bD_0}{K}\right) \left(\frac{\sigma_{\text{imp}}}{G}\right)^n \exp\left(-\frac{Q}{RT}\right) \quad (2)$$

where φ is punch diameter, C_1 and C_2 are material constants, $C_1 \approx 3$ and $C_2 \approx 1$ for wide range of materials.

In Eq. (2), the stress exponent, n , is the slope of $\ln(V_{\text{imp}}T/G) - \ln(\sigma_{\text{imp}}/G)$ plot at a constant temperature. In a similar way, the activation energy Q can be evaluated from a plot of $\ln(V_{\text{imp}}T/G)$ versus $1/T$ at constant σ_{imp}/G .

Figure 7 illustrates the obtained stress exponents for four alloys at 445–475 K. It is clear that the stress exponent values (6.04–6.89) are close to each other. This relative stability of stress exponent with increasing the temperature can be related to high thermal stability of two mean phases: Mg_2Ca and Ca-Mg-Sn which plays key role in the stability of microstructure.

Figure 8 shows the activation energy for all alloys under constant normalized stresses. The obtained activation energy is in the range from 101.37 to 113.8 kJ/mol, while the activation

energies were reported in the range from 92 (pipe diffusion) to 135 kJ/mol (lattice self-diffusion of Mg) [17,18].

Dislocation climb mechanism has been frequently reported as the dominant mechanism for the creep deformation of magnesium based alloys at temperatures between 373 and 523 K under the applied stress in the range of 40–80 MPa [8,18]. For this mechanism, n varies between 4 and 6 and Q is equal to the activation energy for self-diffusion through the lattice. In addition, stress exponent value of 7 has been attributed to the pipe diffusion climb controlled dislocation creep, in which activation energy is equal to that of pipe diffusion [17,29,30]. Comparing the obtained stress exponents (6.04–6.89) and the activation energies (101.37–113.8 kJ/mol) in this study with the literatures [17,18] indicates that the pipe diffusion climb controlled dislocation creep is the dominant mechanism during creep of the alloy.

3.4 Microstructure after impression creep test

Some specimens were cut in half and prepared for the microstructural analysis to study different

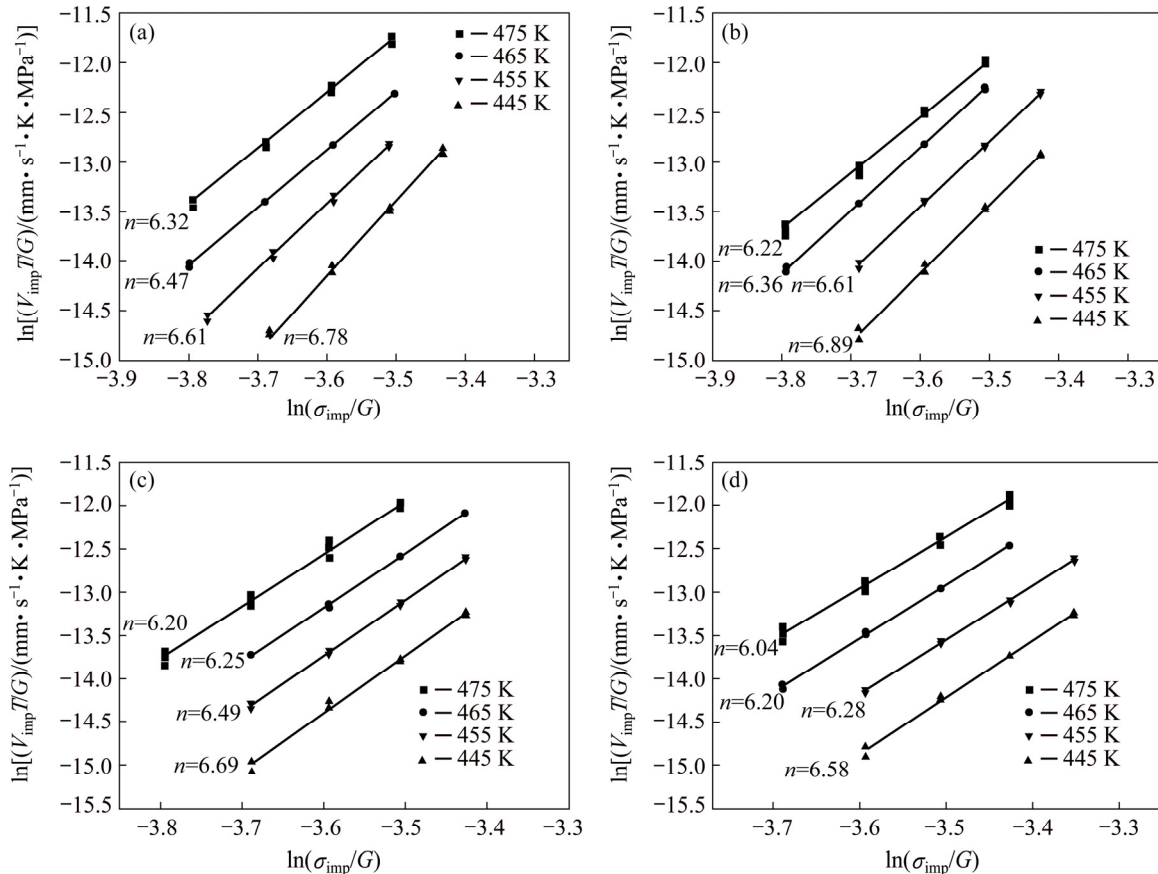


Fig. 7 Variation of $\ln(V_{\text{imp}}T/G)$ with $\ln(\sigma_{\text{imp}}/G)$ of different alloys at constant temperatures for determining stress exponent n : (a) Mg–4Sn; (b) Mg–4Sn–2Ca; (c) Mg–4Sn–3Ca; (d) Mg–4Sn–4Ca

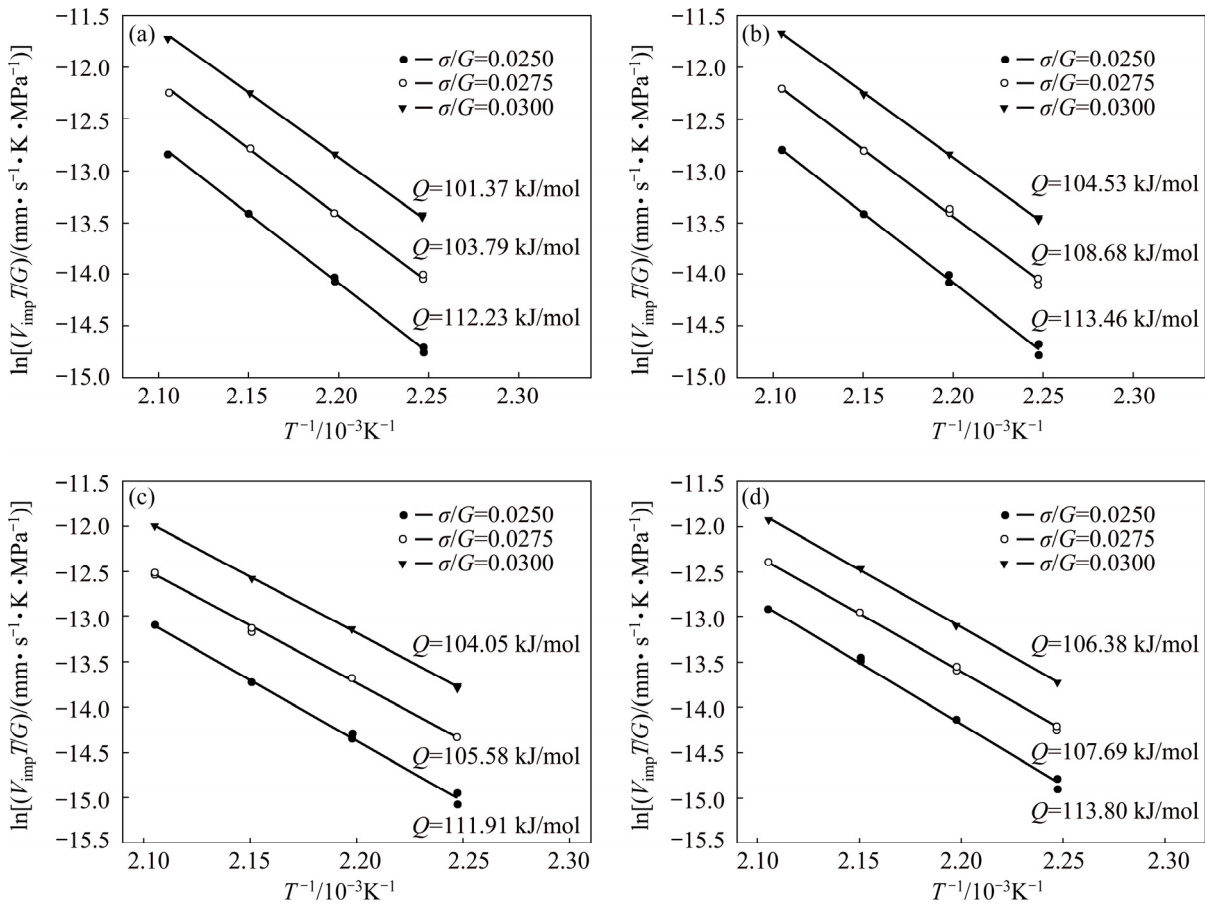


Fig. 8 Variation of $\ln(V_{imp} T/G)$ with $1/T$ of different alloys under constant normalized stresses for determining Q values: (a) Mg-4Sn; (b) Mg-4Sn-2Ca; (c) Mg-4Sn-3Ca; (d) Mg-4Sn-4Ca

sample's zones under the indenter. Figure 9 presents the SEM image of the cross-section of impression edges for the Mg-4Sn-3Ca alloy after impression creep test at 455 K. As shown in Fig. 9, three separated areas are distinguished. The first and

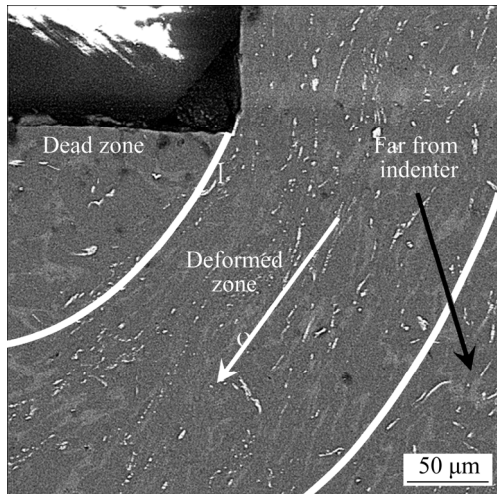


Fig. 9 SEM image of cross-section of impression edges for Mg-4Sn-3Ca alloy after impression creep test at 455 K (Flow direction is indicated by black arrow)

spherical area just below the indenter is a dead zone where interestingly there is no microstructural change. The second area is a wide-spreading and highly deformed zone where the microstructure is changed under extensive shear stress and a flow pattern is observed. In the last zone, which is far away from the indenter, there is no noticeable evolution in phases [10,20,29].

4 Conclusions

(1) The as-cast microstructure of Mg-4Sn alloy consists of $\alpha(Mg)$ matrix and Mg_2Sn intermetallic phases. The addition of Ca more than 2 wt.% suppresses Mg_2Sn formation at the grain boundaries, and instead promotes formation of Ca-Mg-Sn and Mg_2Ca compounds at the grain boundaries.

(2) The creep properties of Mg-4Sn alloy were significantly improved by adding Ca due to the elimination of Mg_2Sn phase and promoting the formation of Ca-Mg-Sn with high thermal stability

and Mg₂Ca distributed continuously at grain boundaries.

(3) The stress exponent, n , was found to be in the range of 6.04–6.89 and activation energy, Q , was obtained between 101.37 and 113.8 kJ/mol for the studied four alloys. These values indicate that the pipe diffusion climb controlled dislocation creep was the dominant creep mechanism.

References

- [1] KIM B H, KIMURA H, PARK Y H, PARK I M. The effect of cerium on microstructures and mechanical properties of Mg–4Al–2Sn–1Ca alloy [J]. *Materials Transactions*, 2010, 51: 1346–1349.
- [2] WAN Xiao-feng, NI Hong-jun, HUANG Ming-yu, ZHANG Hua-li, SUN Jian-hua. Microstructure, mechanical properties and creep resistance of Mg–(8%–12%)Zn–(2%–6%)Al alloys [J]. *Transactions of Nonferrous Metals Society of China*, 2013, 23: 896–903.
- [3] TERADA Y, SATO T. Assessment of creep rupture life of heat resistant Mg–Al–Ca alloys [J]. *Journal of Alloys and Compounds*, 2010, 504: 261–264.
- [4] GERANMAYEH A R, MAHMUDI R. Compressive and impression creep behavior of a cast Mg–Al–Zn–Si alloy [J]. *Materials Chemistry and Physics*, 2013, 139: 79–86.
- [5] PIGARELLI S. Constitutive equations in creep of Mg–Al alloys [J]. *Materials Science and Engineering A*, 2008, 492: 153–160.
- [6] SADDOCK N D, SUZUKI A, JONES J W, POLLOCK T M. Grain-scale creep processes in Mg–Al–Ca base alloys: Implications for alloy design [J]. *Scripta Materialia*, 2010, 63: 692–697.
- [7] SATO T, KRAL M V. Microstructural evolution of Mg–Al–Ca–Sr alloy during creep [J]. *Materials Science and Engineering A*, 2008, 498: 369–376.
- [8] MAZRAE SHAHI E M, NAMI B, MIRE SMAEILI S M. Investigation on the impression creep properties of a cast Mg–6Al–1Zn magnesium alloy [J]. *Materials & Design*, 2013, 51: 427–431.
- [9] WEI S H, CHEN Y G, TANG Y B, ZHANG X P, LIU M, XIAO S, ZHAO Y H. Compressive creep behavior of Mg–Sn–La alloys [J]. *Materials Science and Engineering A*, 2009, 508: 59–63.
- [10] NAYYERI G, MAHMUDI R. The microstructure and impression creep behavior of cast Mg–5Sn– x Ca alloys [J]. *Materials Science and Engineering A*, 2010, 527: 2087–2098.
- [11] PODDAR P, SAHOO K L, MUKHERJEE S, RAY A K. Creep behaviour of Mg–8%Sn and Mg–8%Sn–3%Al–1%Si alloys [J]. *Materials Science and Engineering A*, 2012, 545: 103–110.
- [12] GIBSON M A, FANG X, BETTLES C J, HUTCHINSON C R. The effect of precipitate state on the creep resistance of Mg–Sn alloys [J]. *Scripta Materialia*, 2010, 63: 899–902.
- [13] LIU Hong-mei, CHEN Yun-gui, TANG Yong-bai, WEI Shang-hai, NIU Gao. The microstructure, tensile properties, and creep behavior of as-cast Mg–(1–10)%Sn alloys [J]. *Journal of Alloys and Compounds*, 2007, 440: 122–126.
- [14] HASANI G H, MAHMUDI R. Tensile properties of hot rolled Mg–3Sn–1Ca alloy sheets at elevated temperatures [J]. *Materials & Design*, 2011, 32: 3736–3741.
- [15] WANG W Y, SHANG S L, WANG Y, MEI Z G, DARLING K A, KECSKES L J, MATHAUDHU S N, HUI X D, LIU Z K. Effects of alloying elements on stacking fault energies and electronic structures of binary Mg alloys: A first-principles study [J]. *Materials Research Letters*, 2014, 2: 29–36.
- [16] RASHNO S, NAMI B, MIRE SMAEILI S M. Impression creep behavior of a cast MRI153 magnesium alloy [J]. *Materials & Design*, 2014, 60: 289–294.
- [17] LIU Hong-mei, CHEN Yun-gui, TANG Yong-bai, HUANG De-ming, NIU Gao. The microstructure and mechanical properties of permanent-mould cast Mg–5wt.%Sn–(0–2.6)wt.%Di alloys [J]. *Materials Science and Engineering A*, 2012, 545: 103–110.
- [18] MO N, TAN Q Y, BERMINGHAM M, HUANG Y D, DIERINGA H, HORT N, ZHANG M X. Current development of creep-resistant magnesium cast alloys: A review [J]. *Materials & Design*, 2018, 155: 422–442.
- [19] HUANG Y D, DIERINGA H, KAINER K U, HORT N. Deformation-induced dynamic precipitation during creep in magnesium-tin alloys [J]. *Key Engineering Materials*, 2015, 627: 365–368.
- [20] KHALILPOUR H, MIRE SMAEILI S M, BAGHANI A. The microstructure and impression creep behavior of cast Mg–4Sn–4Ca alloy [J]. *Materials Science and Engineering A*, 2016, 652: 365–369.
- [21] LI W D, HUANG X F, HUANG W G. Effects of Ca, Ag addition on the microstructure and age-hardening behavior of a Mg–7Sn (wt.%) alloy [J]. *Materials Science and Engineering A*, 2017, 692: 75–80.
- [22] WEI Shang-hai, CHEN Yun-gui, TANG Yong-bai, LIU Ming, XIAO Su-fen, ZHANG Xiao-ping, ZHAO Yuan-hua. Compressive creep behavior of Mg–Sn binary alloy [J]. *Transactions of Nonferrous Metals Society of China*, 2008, 18(S): s214–s217.
- [23] YANG Ming-bo, MA Yan-long, PAN Fu-sheng. Effects of little Ce addition on as-cast microstructure and creep properties of Mg–3Sn–2Ca magnesium alloy [J]. *Transactions of Nonferrous Metals Society of China*, 2009, 19: 1087–1092.
- [24] YANG Ming-bo, MA Yan-long, PAN Fu-sheng. Comparison of as-cast microstructure, tensile and creep properties for Mg–3Sn–1Ca and Mg–3Sn–2Ca magnesium alloys [J]. *Nonferrous Metals Society of China*, 2010, 20: 584–589.
- [25] SASTRY D H. Impression creep technique—An overview [J]. *Materials Science and Engineering A*, 2005, 409: 67–75.
- [26] FARAJI M, KHALILPOUR H. Effect of phosphorous inoculation on creep behavior of a hypereutectic Al–Si alloy [J]. *Journal of Materials Engineering and Performance*, 2014, 23: 3467–3473.
- [27] KIM D H, LEE J Y, LIM H K, KYEONG J S, KIM W T, KIM D H. The effect of microstructure evolution on the elevated temperature mechanical properties in Mg–Sn–Ca system [J]. *Materials Transactions*, 2008, 49(10): 2405–2413.

- [28] THENAMBIKA V, JAYALAKSHMI S, ARVIND S R, KIRUBA N J, GUPTA M. Impression creep behaviour of extruded Mg–Sn alloy [C]//Proceedings of International Conference on Recent Advancements in Design, Automation and Intelligent Systems. Now York, 2016: 174–178.
- [29] NAMI B, RAZAVI H, MIRDAMADI S, SHABESTARI S G, MIRE SMAEILI S M. Effect of Ca and rare earth elements on impression creep properties of AZ91 magnesium alloy [J]. Metallurgical and Materials Transactions A, 2010, 41: 1973–1982.
- [30] MAHMUDI R, MOEENDARBARI S. Effects of Sn additions on the microstructure and impression creep behavior of AZ91 magnesium alloy [J]. Materials Science and Engineering A, 2013, 566: 30–39.

添加 Ca 对 Mg–4Sn 合金组织演变和蠕变性能的影响

Amir BAGHANI¹, Hamid KHALILPOUR², Seyed Mahdi MIRE SMAEILI³

1. Department of Mechanical Engineering, University of Iowa, Iowa City, IA, USA;

2. Department of Mining, Metallurgical and Materials Engineering, Laval University, Québec, Canada;

3. Faculty of Mechanical Engineering, Shahid Rajae Teacher Training University, Tehran, Iran

摘要: 通过压入蠕变试验, 研究 Ca 添加量(最高达 4%, 质量分数)对 Mg–4Sn 合金的显微组织和蠕变性能的影响。压入蠕变试验的操作温度为 445~475 K, 归一化应力(σ/G , σ 为应力; G 为剪切模量)为 0.0225~0.035。利用光学显微镜和扫描电子显微镜对样品的显微组织进行研究。结果表明, Ca 的加入量大于 2%(质量分数)可抑制较不稳定 MgSn₂ 相的形成, 从而使晶界处形成热稳定性较高的 Ca–Mg–Sn 相和 Mg₂Ca, 提高 Mg–4Sn 合金的抗蠕变性能。根据压入蠕变试验所得的应力指数($6.04 < n < 6.89$)和激活能($101.37 \text{ kJ/mol} < Q < 113.8 \text{ kJ/mol}$)可得出结论: 管扩散攀移控制的位错蠕变是合金主要的蠕变机制。

关键词: 压入蠕变试验; Mg–Sn–Ca 合金; 蠕变机制; 显微组织

(Edited by Wei-ping CHEN)